

# Authors' response file

I.E. Gharamti, J.P. Dempsey, A. Polojärvi and J. Tuhkuri

January 13, 2021

---

## Replies to reviewers' comments

We thank the editor and the reviewers for carefully reviewing our work and making constructive comments. We appreciate all the time and efforts they put in their thorough review. All the reviewer comments were considered in the revised manuscript. Detailed answers to each comment are given below.

### 1. General modifications in the revised manuscript

- Added text is displayed in red.
- Deleted sentences are marked with a red strikethrough.

### 2. Reviewer 1 comments

1. The authors go further, however, weakening/endangering the manuscript. They analyze their data in terms of a constitutive model that was developed by Schapery (1969, 1997) for uniaxial loading (noted in lines 171-173). But in the experiments at hand, deformation occurred under a multiaxial stress state. Given that the model and the data relate to different states of stress and given that values of the many (eight) unknown parameters in the model were derived by fitting the data and not from independent measurements, it is difficult to accept the statement (lines 303-305) that the analysis “ provides a firm support of the ability of Schapery’s constitutive model to describe the time-dependent response of columnar freshwater S2 ice up to crack growth initiation.”

The Schapery model is developed for a uniaxial normal stress state. In our experimental set up (Fig. 1), the response of the test specimen is dominated by the normal stresses at the direction normal to the X-axis, ahead of the crack. This stress state can be approximated as uniaxial in the same way as in beam bending; the stress is uniaxial tension at the crack tip and then changes linearly. Adamson and Dempsey [1] have successfully used the same type of modelling for a similar setup. In addition, Schapery’s model has been verified and validated by LeClair [2]. Other analyses and approaches didn’t do as well. For instance, the experimental data by LeClair [2] was modelled by Schapery’s model [2] and by a physically-based FE model [3]. While the physical model did a reasonable job of modelling the data, Schapery’s straight-forward model did a better job.

The approach we have used – fitting a model with experimental data by using optimization – is common in fracture models with several parameters. Pure experimental methods to determine these parameters have proven extremely difficult and indirect methods, based on parametric fitting, has been developed and used instead [4].

Some text is added in that context.

2. It is even more difficult to accept the claim (lines 242-243) that under the conditions of these experiments “there is no delayed elastic recovery”.

We understand the reviewer’s reluctance to accept the lack of major delayed elastic recovery. What we measured for freshwater ice has not been reported earlier. However, this surprising response of no significant viscoelasticity is what we measured in these tests (Figs 7b and 8b). Further studies are needed to confirm the result and to find explanations for the behaviour. It may be important that, compared with earlier work on freshwater S2 ice, our samples were large and very warm.

3. The title presents a problem: it is misleading. This is not the kind of experiment that allows a characterization of elastic-viscoelastic deformation of ice. Rather, as already noted, it allows a conclusion to be made on fracture toughness and its insensitivity to pre-strain. The title needs to be changed to reflect that finding.

We changed the title into “Creep and fracture of warm columnar freshwater ice” and hope that it reflects the content better than the original title.

4. The other problem is that the manuscript contains a contradiction. The claim that the experiments were performed on ice at  $-2^{\circ}\text{C}$  contradicts the temperature profile shown in Fig. 3a. There, where temperature is plotted versus depth (from 0 to 35 cm) in the ice, temperature ranges from  $-0.3^{\circ}\text{C}$  near the top to  $0^{\circ}\text{C}$  near the bottom.

We apologize for the confusion. During the experiments, the ambient temperature in the laboratory was kept at  $-2^{\circ}\text{C}$ . The temperature profile within the ice is shown in Fig. 2a. The text is edited to clear up this confusion.

5. Finally, it would be helpful to know in which journal the repeated reference to Gharamti et al. is “in press”. The paper by Gharamti et al. [5] is now published. The cited reference is edited.

### 3. Reviewer 2 comments

1. Page 1, line 14 – The eventual goal of these experiments seems to be to better describe or model ice loads during sea ice floe interactions with structures in the Arctic. As the authors mention the deformation modes are quite complex during ice-structure interaction, but there is no literature cited on this work. For example, Claude Daley at MUN has done experimental and modeling work on this using ice indentation experiments on structures, which seems to be the most relevant mechanism for transfer of ice loads onto structures. One would rarely imagine a floating ice flow to be subjected to mode I tension. Please add more description to the introduction about what experimental data is available, what motivated the current experimental study and why mode I fracture experiments are relevant in the context of ice-structure interaction.

Many of the comments by the reviewer deal with sea ice, Arctic and engineering relevance. It appears that the introduction of our submission was unfortunately giving an impression that our work on creep deformation and fracture of freshwater ice has direct application in sea ice and Arctic engineering. That is not the case and we

apologize for the confusion caused. Deformation and fracture of ice are highly dependent on salinity, temperature, strain rate, sample size, grain type, and grain size. Our paper reports results from laboratory experiments which were conducted to study the creep and fracture of warm, floating, columnar grained S2 freshwater ice. The work is directly relevant to a number of practical problems on columnar freshwater ice [6]. However, it has also general relevance to the creep and fracture of a quasi-brittle material. Unless we restrict our interest on the short time scales where only elastic response is relevant, the creep deformations must be modeled to obtain the true fracture behavior. In materials with time-dependent properties, the fracture and creep deformations are coupled.

Mode I loading is rather common in a number of ice problems. For example, freshwater ice sheets fracture when in contact with ships, river ice fractures during interaction with bridge piers, and thermal cracks form in lakes and reservoirs.

2. Page 2, line 26 – Why has it become increasingly important to use time-dependent constitutive modeling. When was it less important? Perhaps, the authors are referring to recent drastic changes in the Arctic sea ice. The sentence here is rather vague.

We did think of the warming climate and thus warming ice which may potentially increase the importance of creep deformation and apologize for not writing this clearly. In addition, the applications like river ice breakup happen in late spring and the ice is very warm. For that reason, the creep deformations are very important but historically cold ice has been studied typically.

3. Page 2, line 30 – While it is true that ice sheet and glacier modelers use viscous creep law, the terms long term and short term are vaguely defined. As my research has found, sometime a few hours is all that takes for viscous behavior to dominate, which is not really that long term. Please explain clearly that short time scales you mean are seconds or minutes or hours.

We agree that “long” and “short” are vaguely defined terms and have different meaning in different contexts. The text is edited. It is also not correct to imply that this study is relevant to glaciers. We are studying columnar grained ice not very fine grained equiaxed snow ice.

4. Page 3, lines 65 to 70 – The study’s aims are noted here. However, there is an important discussion missing here about viscoelastic fracture mechanics. The concept of fracture toughness or critical stress intensity factor is only well defined for linear elastic solids or elasto-plastic solids with small scale yielding. The authors should state and explain the definitions. Of the apparent fracture toughness  $K_Q$  and the loading rate  $\dot{K}$ , and why they are relevant quantity to ice mechanical behavior. What are the specific assumptions made about the ice viscoelastic behavior. Refer to any experiments and modeling studies in the literature that establish the theory of fracture in time-dependent materials.

We added a discussion on time-dependent fracture. The reviewer is correct. It has been known that the viscoelastic fracture mechanics [7] is on a firm foundation so long as a finite cohesive zone is attached to the traction-free crack tip. The one-parameter fracture mechanics encompassed by the  $K_Q$  notation is not applicable [8] and is removed. Although  $\dot{K}$  was used for comparative measure of the loading rate, it is replaced by the measured time of failure in each

experiment. The  $K_Q$  plot is replaced by a plot of the peak loads. We hope that any confusion will be cleared up then.

5. Page 3, lines 75 to 85 – The scale of these experiments is truly impressive, however, referring to my previous why is mode I fracture relevant for ice-structure interaction. Aren't sea ice floes breaking up due to compression and plate buckling processes. Please explain the motivation for these experiments and how it can be used in largescale modeling of ice-floe structure interaction. For example, will this study provide necessary parameters for discrete element modeling of sea ice-structure or ice-ship interaction.

Please see our response to Comment 1. Our main concern here is how tensile cracks develop in columnar freshwater ice under the applied loading.

6. Page 3, line 85 – The top surface temperature is noted as -2 C, but in Figure 2a the temperature below the surface is around -0.3 C. I am confused, please explain.

We apologize for the confusion. During the experiments, the ambient temperature in the laboratory was kept at -2°C. The temperature profile within the ice is shown in Fig. 2a. The text is edited to clear this confusion.

7. Page 3, line 86 – Please provide some more description of the experimental setup, ice growth etc as we still do not have access to your paper in press. Why does the grain size increase with depth? Also, how realistic is this for sea ice as opposed to stagnate lake ice with no waves.

The paper by Gharamti et al. [5] is now published. The cited reference is edited.

The grain size increasing with depth is the characteristic of columnar ice [9]. Cole [10] wrote: “In columnar ice, the average grain diameter in the horizontal plane typically increases with depth because the faster growing, c-axis horizontal grains systematically eliminate the grains least favorably oriented for growth.”

Michel and Ramseier [9] classified lake and river ice according to the size, shape and orientation of the crystals and the environmental factors causing them. For quiet lakes subject to no wind and no snow falling, S1 ice with vertical c-axis orientation will form. The paper will be revised with a thorough discussion of the microstructure (grain size effect).

8. Page 3, line 90 – The experiments report the load values and peak loads. However, it would be useful from a modeling perspective to get crack initiation stress. Is it possible that this sort of information can be extracted and reported from experiments. This will make the paper's results useful to those modeling sea ice-structure interaction. We cannot determine the crack-initiation stress in these creep and cyclic-recovery experiments. The crack-initiation stress can be computed for the monotonic DC tests [5] because the stress-separation curve was derived for the DC tests. However, for the LC tests here, the stress-separation curve is unknown.

9. Page 4, line 95 – How do the applied load rates and load levels related to real ice floes. A bit more justification is needed to establish the rationale for testing.

We are mainly concerned here with the tensile cracks growing in columnar freshwater ice. We could be studying the bearing capacity of lake ice, the splitting of lake ice by an ice breaker, the breakup of river ice, etc. Ice in nature is

loaded through a wide range of time scales. The loading was chosen to reflect one time-dependent response that can be encountered. The loading rate used is similar than used in earlier sea ice studies and thus allows comparison of these two materials.

10. Page 4, line 103 – I am failing to understand the purpose of creep loadings. If the creep loads were kept small so that no damage nucleates and with recovery periods, there should not affect. In fact, this is what is observed with the results.

The creep-recovery tests in the time-domain were conducted to study the response of the ice under several load steps, which has not been studied before on freshwater ice. Previous studies have concentrated either on cyclic loading in the frequency domain [11, 12] or on a single load step [13].

The main reason the loads were kept small is to avoid damage because we are not modelling damage [14]. The creep/cyclic-recovery sequence did affect the accumulation of the viscoplastic component of the crack opening displacement (Fig. 11).

11. Page 4, line 108 – Once again how do these cyclic load levels and loading rates related to the physical setting. Are these in any way representative of the ocean wave loads on sea ice floes?

Please see our response to Comment 9.

12. Page 5, Equation 2 – Replacing the stress and strain with load and displacement is valid only for linear behavior. Has Schapery’s model used with load and displacement before in any literature?

The same modelling for load and displacement has been used by Adamson and Dempsey [1]. The modelling works very well, and the CMOD was predicted correctly until the crack began to propagate.

13. Page 7, line 195 – What is the purpose of the modeling and parameter estimation. I ask this because I work in ice fracture modeling and cannot really see how these experiments can improve the fracture models.

The approach we have used – fitting a model with experimental data by using optimization – is common in fracture models with several parameters. Pure experimental methods to determine these parameters have proven extremely difficult and indirect methods, based on parametric fitting, has been developed and used instead [4]. In addition, the Schapery model can fit successfully both creep-recovery and cyclic loading.

14. Page 7, line 204 – How is the weight function approach applied? Numerical evaluation of integrals with weight function approach can lead to inconsistencies. Why not use the displacement correlation method directly using COD and CMOD and NCOD?

A lot of work has been done on the weight function of an edge-cracked rectangular plate [15] used in the current experiments. The accuracy of this weight function was derived, assessed and thoroughly validated by comparison with other published data. The displacement correlation method cannot be used because of the presence of creep. The deformations are affected by creep and by possible growth of the crack.

15. Page 8, line 213 – Figure 5a needs more explanation. In viscoelastic materials, the peak load increases with loading rate. Please define precisely what  $\dot{K}$  is and why the peak load decreases as you increase  $\dot{K}$ . Also, defined what you mean by failure load. Is it the same as peak load? If so, then just use one terminology consistently. In these experiments, the failure load is the same as the peak load. We are not including  $K$  and  $\dot{K}$  in the analysis anymore.

16. Page 8, line 228 – What are the differences in the post-peak load curves that should be identified. Is it the oscillatory nature of load displacement curves in cyclic sequences? A better explanation would be useful.

The decay of the load for the creep-recovery tests (Fig. 5b) took a much longer time than that for the monotonic tests (Fig. 5a). Unfortunately, the reason for the oscillatory nature of the signal is unclear to us.

17. Page 8, line 235 – The authors state “It is clear from Figs. 7b and 8b : : :” How is it clear? The writing style is a bit confusing.

The measured displacement records in Figs. 7b and 8b show no significant viscoelastic component. A typical creep displacement-time record displaying the three displacement components (elastic, viscoelastic and viscous) looks as shown in Fig. 1. By simply comparing Fig. 1 here with each creep/cyclic-recovery sequence in Figs. 7b and 8b in the manuscript, one can deduce that the viscoelastic displacement and the viscoelastic recovery were not significant.

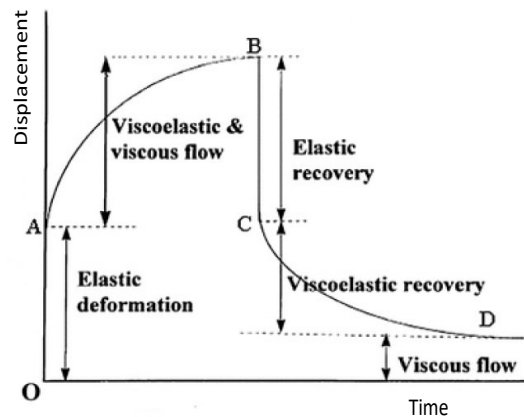


Figure 1: General displacement-time record for a creep-recovery test. The elastic, viscoelastic, and viscous (viscoplastic) components are marked.

18. Page 9, line 243 – I only know of the Maxwell model and the generalized Maxwell model. What is a simple Maxwell model?

We meant a Maxwell model composed of a nonlinear spring and a nonlinear dashpot. The word “simple” is deleted.

19. Page 9, lines 247 to 259 – This whole paragraph should be written as a separate discussion section. Based on my recollection the experiments of Sinha and Cole involved compression loads and not tension loads, and there were not really on pre-cracks ice slabs. This lead to the question on why delayed elastic effect was not there? However, it is not clear why this is even an important question in the context of ice-structure interaction.

The authors thank the reviewer for his/her recommendation. The authors created a separate discussion section.

20. Page 267 – The statement “When the specimen dimensions are several meters, apparently viscoelasticity is not an important deformation component” is poorly explained. Also, what is the consequence of this finding? Is the author suggestion that one can just use elastic model for sea ice-interaction? Is there any relevance of these results for floating ice shelves, which are much larger than ice floes?

Our experiments suggest that for the large sample size and the kind of ice studied (very warm freshwater ice) under the loading applied, the response was elastic-viscoplastic. More experiments are needed to make more general conclusions.

21. Overall, I am not clear on what the broader purpose of the paper is? Why did the author’s select the specimen size and loading rates they used. Why specifically test creep/cyclic recovery? How is this work relevant to the motivation mentioned in the first paragraph of the introduction – interaction of ice floes with structure. How to use the data and findings of this paper in any future modeling analysis. A comprehensive revision of this article is needed and I recommend including a discussion section to address the implications of this research.

Please see our response to Comment 1.

## References

1. Adamson RM, Dempsey JP. Field-scale in-situ compliance of arctic first-year sea ice. *Journal of Cold Regions Engineering* 1998;12:52–63.
2. LeClair ES, Schapery RA, Dempsey JP. A broad-spectrum constitutive modeling technique applied to saline ice. *International Journal of Fracture* 1999;97:209–26.
3. O’Connor D, West B, Haehnel R, Aseath-Smith E, Cole D. A viscoelastic integral formulation and numerical implementation of an isotropic constitutive model of saline ice. *Cold Regions Science and Technology* 2020;171:102983.
4. Elices M, Guinea GV, Gomez J, Planas J. The cohesive zone model: advantages, limitations and challenges. *Engineering Fracture Mechanics* 2002;69:137–63.
5. Gharamti IE, Dempsey JP, Polojärvi A, Tuhkuri J. Fracture of S2 columnar freshwater ice: size and rate effects. *Acta Materialia* 2021;202:22–34.
6. Ashton GD. River and lake ice engineering. Water Resources Publication, Littleton, Colorado; 1986.
7. Kostrov BV, Nikitin LV. Some general problems of mechanics of brittle fracture. *Archiwum Mechaniki Stosowanej* 1970;22, English Version:749–76.
8. Dempsey JP, Cole DM, Wang S. Tensile fracture of a single crack in first-year sea ice. *Philosophical Transactions of the Royal Society A* 2018;376(2129):20170346.
9. Michel B, Ramseier R. Classification of river and lake ice. *Canadian Geotechnical Journal* 1971;8(1):36–45.

10. Cole DM. The microstructure of ice and its influence on mechanical properties. *Engineering Fracture Mechanics* 2001;68(17-18):1797–822.
11. Cole DM. Reversed direct-stress testing of ice: Initial experimental results and analysis. *Cold Regions Science and Technology* 1990;18:303–21.
12. Cole DM. A model for the anelastic straining of saline ice subjected to cyclic loading. *Philosophical Magazine A* 1995;72(1):231–48.
13. Sinha NK. Rheology of columnar-grained ice. *Experimental Mechanics* 1978;18:464–70.
14. Kachanov L. Introduction to continuum damage mechanics; vol. 10. Springer Science & Business Media; 1986.
15. Dempsey JP, Mu Z. Weight function for an edge-cracked rectangular plate. *Engineering Fracture Mechanics* 2014;132:93–103.



# ~~Elastic-viscoplastic characterization of S2 columnar freshwater ice~~ **Creep and fracture of warm columnar freshwater ice**

Iman E. Gharamti<sup>1</sup>, John P. Dempsey<sup>2</sup>, Arttu Polojärvi<sup>1</sup>, and Jukka Tuhkuri<sup>1</sup>

<sup>1</sup>Department of Mechanical Engineering, Aalto University, Espoo 00076, Finland

<sup>2</sup>Department of Civil and Environmental Engineering, Clarkson University, Potsdam, NY 13699, USA

**Correspondence:** Iman E. Gharamti (iman.elgharamti@aalto.fi)

**Abstract.** This work addresses the time-dependent response of 3m x 6m floating edge-cracked rectangular plates of columnar freshwater S2 ice, by conducting load control (LC) mode I fracture tests at ~~-2 C~~ in the Ice Tank of Aalto University. **The thickness of the ice plates was about 0.4m and the temperature at the top surface about -0.3 C.** The loading was applied in the direction normal to the columnar grains and profile consisted of creep/cyclic-recovery sequences followed by a monotonic ramp to fracture. The LC test results were compared with previous monotonically loaded displacement control (DC) experiments of the same ice, and the effect of creep and cyclic sequences on the fracture properties were discussed. To characterize the nonlinear displacement-load relation, Schapery's constitutive model of nonlinear thermodynamics was applied to analyze the experimental data. A numerical optimization procedure using Nelder-Mead's (N-M) method was implemented to evaluate the model functions by matching the displacement record generated by the model and measured by the experiment. The accuracy of the constitutive model is checked and validated against the experimental response at the crack mouth. Under the testing conditions, the creep phases were dominated by a steady phase, and the ice response was **overall** elastic-viscoplastic; no **significant** viscoelasticity or major recovery were detected. In addition, there was no clear effect of the creep loading on the fracture properties **at crack growth initiation**: the ~~apparent fracture toughness~~, failure load, and crack opening displacements.

## 1 Introduction

~~The interaction of ice floes with structures is a major challenge for all operations. Understanding the mechanics of ice-structure interaction is very important to ensure the safe design and secure operations of ships and offshore structures. This interaction phenomenon involves complicated physical processes and combined deformation modes that should be analyzed in order to answer several engineering questions: such as estimating the ice loads on structures and the necessary forces required for fracturing and navigating through an ice sheet.~~

~~Tackling this problem is handicapped by the wide range of time, rate and load scales involved. Ice response is highly dependent on the loading conditions. At high deformation rates, ice behaves in a brittle manner, and fracture controls the loads exerted on structures. At low deformation rates, ice creeps, and the forces are controlled by time-dependent deformation (Palmer et al., 1983; Gharamti et al., 2021). In fact, ice can exhibit a strong time-dependent behavior depending on the operating factors: loading profile, load levels, duration of load/unload applications, temperature, and other environmental factors. Accordingly,~~

25 precise prediction of ice forces requires an analysis that simultaneously accounts for the time-dependent and fracture behavior of ice.

~~The time-dependent constitutive modeling has become increasingly important to characterize the mechanical behavior of ice. The time-dependent response of ice is highly nonlinear, and the constitutive model should incorporate elastic, viscoelastic/delayed elastic (time-dependent and recoverable) and viscoplastic/viscous (time-dependent and unrecoverable) components, depending on the engineering problem. For example, glaciologists are interested solely in long term creep behavior, hence an ice model to them is simply a viscous creep law. Floating ice problems generally focus on shorter term behavior with damage/failure so all three components of deformation need to be modeled.~~

Understanding the deformation and fracture processes of columnar freshwater ice is important in many engineering problems. For example, freshwater ice sheets fracture when in contact with ships, river ice fractures during interaction with bridge piers, and thermal cracks form in lakes and reservoirs. Deformation and fracture processes of freshwater ice are highly dependent on temperature, strain rate, sample size, grain type and grain size. Qualitatively, high temperature and low strain rate lead to viscous behaviour and ductile fracture; low temperature and high strain rate lead to elastic behaviour and brittle fracture (Gharamti et al., 2021). However, quantitatively these relations are not well known.

As the response of freshwater ice is time-dependent, a general constitutive model should incorporate elastic (immediate and recoverable), viscoelastic (or delayed elastic, time-dependent and recoverable) and viscoplastic (time-dependent and unrecoverable) components (Jellinek and Brill, 1956; Sinha, 1978). The importance of each component depends on the problem studied. For example, thermal deformations of ice in dams can have a time scale of a few days and creep behaviour dominates. In ice-structure interaction problems, the time scale of interest is often seconds and hours, so all three components of deformation need to be modeled.

45 This paper reports results from laboratory experiments which were conducted to study the time-dependent response and fracture of columnar freshwater ice. The work is directly relevant to a number of practical problems (Ashton, 1986), but has also general relevance in ice research by studying the coupled creep and fracture in a quasi-brittle material. Unless just short time scales are involved, where only elastic response is relevant, the creep deformations must be modeled to obtain the true fracture behavior. In materials with time-dependent properties, the fracture and creep responses are coexistent.

50 The time-dependent behavior of freshwater ice has been addressed with great attention, and several constitutive models were developed (Michel, 1978; Sinha, 1978; Le Gac and Duval, 1980; Ashby and Duval, 1985; Sunder and Wu, 1989; Mellor and Cole, 1983; Cole, 1990; Duval et al., 1991; Sunder and Wu, 1990; Abdel-Tawab and Rodin, 1997; Santaoja, 1990). Constitutive laws can be phenomenological or micromechanical. Micromechanical modeling in ice faces challenges because the characterization of the microscopic mechanisms of ice deformation is still inadequate (Abdel-Tawab and Rodin, 1997).

55 Phenomenological laws are classified into two groups. The first group are empirical-based relations (Sinha, 1978; Schapery, 1969). Their equations relate macroscopic variables: stress/load, strain/displacement, and time. They do not contain state variables that describe the internal state of the material and are valid only for constant stress/load. The functions in these models can be easily calibrated to simulate the experiments. The second group of phenomenological models starts from physically-based models involving internal state variables (dislocation density, internal stresses reflecting hardening, etc ...); they develop

60 differential equations for the evolution of these variables with time and quantify the dependence of these variables on stress, temperature and strain (Le Gac and Duval, 1980; Sunder and Wu, 1989, 1990; Abdel-Tawab and Rodin, 1997). These models provide insights into the microscopic mechanisms taking place, and the state variables describe the deformation resistance offered by changes in the microstructure of the material. However, they require a proper identification of the deformation mechanisms.

65 The effect of time-dependent loading on the strength of freshwater ice has been examined in the literature. Subjecting freshwater ice to cyclic loading apparently leads to a significant increase in the tensile, compressive, and flexural strength of that ice (Murdza et al., 2020; Iliescu et al., 2017; Iliescu and Schulson, 2002; Cole, 1990; Jorgen and Picu, 1998). On the other hand, no detailed investigation of the effect of creep and cyclic loading on the fracture properties of freshwater ice has been conducted in the past.

70 ~~The goal of this paper is to characterize the time dependent and fracture behavior of 3m x 6m floating edge-cracked rectangular plates of columnar freshwater S2 ice under creep-recovery loading and monotonic loading to fracture at -2 C. A program of five load control (LC) mode I fracture tests was completed in the test basin (40 m square and 2.8 m deep) at Aalto university. Creep and cyclic sequences were applied below the failure loads, followed by monotonic ramps leading to complete fracture of the specimen. The LC results were compared with the fracture results of monotonically loaded displacement control (DC) tests of the same ice (Gharamti et al., 2021), and the effect of the creep and cyclic sequences on the fracture properties were analyzed.~~

Laboratory experiments were conducted to measure the time-dependent response and fracture behavior of 3m x 6m floating edge-cracked rectangular plates of columnar freshwater S2 ice, loaded in the direction normal to the columnar grains. The ice studied was warm, the temperature at the top surface of the samples was about -0.3 °C. Compared to earlier studies with  
80 freshwater ice, the samples were large (3m x 6m) and very warm. A program of five load control (LC) mode I fracture tests was completed in the test basin (40 m square and 2.8 m deep) at Aalto University. Creep/cyclic-recovery sequences were applied below the failure loads, followed by monotonic ramps leading to complete fracture of the specimen. The LC results were compared with the fracture results of monotonically loaded displacement control (DC) tests of the same ice (Gharamti et al., 2021), and the effect of the creep and cyclic sequences on the fracture properties were analyzed.

85 The constitutive modeling used in this paper was presented by Schapery Schapery (1969) and, where it was applied to polymers. Schapery's model belongs to the first phenomenological group and originates from the theory of nonlinear thermodynamics. This study presents the first attempt to use Schapery's model for freshwater ice. The choice of this model for freshwater ice is motivated by the fact that the model was successfully applied to saline ice (Schapery, 1997; Adamson and Dempsey, 1998; LeClair et al., 1999, 1996) with encouraging results. The model accurately described the deformation response  
90 during load/unload applications over varying load profiles.

The experiments in this study aim to assess the time-dependent nature of warm columnar freshwater S2 ice. Especially, the study aims to examine: 1) the extent to which the elastic, viscoelastic and viscoplastic components **contribute to the ice deformation as defined through the crack mouth opening displacement** ~~contribute to the crack mouth opening displacement~~, 2) the effects of the testing conditions on the creep stages (primary/transient and steady-state/secondary) present in the ice, 3)

95 the effects that creep and cyclic sequences have on the fracture properties; i.e. ~~apparent fracture toughness~~, failure load and crack growth initiation displacements, and 4) the ability of Schapery's nonlinear constitutive model to predict the experimental response.

The rest of the paper is structured as follows. In Section 2, a description of the experimental setup, testing conditions, and the applied loading profile is presented. Section 3 introduces Schapery's model that is used to analyze the experiments. In section 100 4, the experimental and model results are summarized and analyzed. Section 5 concludes the paper.

## 2 Creep-recovery fracture experiments

### 2.1 Experimental details

The ice specimens tested were 3m x 6m rectangular plates, cut from a 40m x 40m parent sheet, with a thickness of 340 - 410 mm, and instrumented as shown in Fig. 1. ~~The experiments were conducted at an ambient temperature of -2 C.~~ The ice 105 was columnar freshwater S2 ice having a mean grain size of 6.5 mm (Fig. 2b). ~~The temperature at the top surface was about -0.3 C, as shown in Fig. 2a.~~ An edge crack of length  $A_0$  ( $A_0 \approx 0.7 L$ ) was cut and tip-sharpened in each ice specimen. The response of the ice was monitored by using a number of surface-mounted linear variable differential transducers (LVDTs). LVDTs were placed at five different locations along the crack to measure directly the crack opening displacements. Fig. 1 labels these positions as CMOD, COD, NCOD1, NCOD2, and NCOD3 for the crack mouth, intermediate crack, 10 cm behind 110 the initially sharpened tip, 10 cm ahead of the tip, and 20 cm ahead of it, respectively. A hydraulically operated device was inserted in the mouth of the pre-crack to load the specimen ~~horizontally, in the direction normal to the columnar grains~~, with a contact loading length of 150 mm, denoted by  $D$  in Fig. 1. The tests were load controlled by a computer-operated closed-loop system that also recorded the displacement measurements. ~~Creep/cyclic-recovery sequences were applied below the failure loads, followed by monotonic ramps leading to complete fracture of the specimen. The loading rate used is similar than used in earlier sea ice studies (LeClair et al., 1999; Adamson and Dempsey, 1998) and thus allows comparison of these two materials.~~ 115 ~~The experiments were conducted with warm ice, -2 C at the top surface as shown in Fig. 2a.~~ The global behavior of the crack propagation was straight through the gauges. Detailed description of the experimental setup, ice growth, microstructure, and fractographic analysis is provided in (Gharamti et al., 2021).

### 2.2 Creep-recovery and monotonic loading profile

120 In two tests, ice specimens were subjected to creep-recovery loading followed by a monotonic fracture ramp. The creep-recovery sequences consisted of four constant load applications, separated by zero load recovery periods. Each sequence was composed of alternating load/hold and release/recovery periods. Creep phases were applied at load levels of 0.4 kN, 0.8 kN, 1.2 kN, and 0.4 kN, as given by the loading signal in Fig. 3a. The loads were chosen low enough to avoid crack propagation and failure of the specimen. Each load-hold-unload was applied in the form of a trapezoidal wave function to avoid instantaneous 125 load jump and drop; the load up was applied in approximately 10 seconds and released in approximately 10 seconds. The

slopes of the wave on load up and load release were 0.04kN/s, 0.08 kN/s, and 0.12 kN/s for the 0.4kN, 0.8 kN, and 1.2 kN load levels, respectively.

Once at the desired hold level, the load was kept constant for a predetermined time interval. The load intervals were multiples of the hold interval for the 0.4 kN load level,  $\Delta t_1 = 126$  seconds. For the 0.8 kN and 1.2 kN load levels, the time interval was  
130 doubled and quadrupled:  $2\Delta t_1 = 252$  seconds and  $4\Delta t_1 = 504$  seconds, respectively. The four zero load recovery periods, separating the creep load periods, were also function of  $\Delta t_1$ . Three recovery periods were held at zero load level for  $5\Delta t_1 = 630$  seconds, but the last recovery period was maintained for a longer interval of  $10\Delta t_1 = 1260$  seconds.

Immediately following the creep and recovery loading sequences, the specimen was loaded monotonically to failure on a load-controlled linear ramp. The ramp up to the peak load and unloading were each applied over an interval of  $\Delta t_1$ .

### 135 2.3 Cyclic-recovery and monotonic loading profile

In three tests, ice specimens were loaded with cyclic-recovery sequences followed by a fracture ramp, as shown in Fig. 3b. The cyclic-recovery loading consisted of 3 sequences, each being composed of four fluctuating loads, at the levels of 0.4 kN, 0.8kN, and 1.2 kN. Each cyclic sequence continued for a constant time interval  $\Delta t_2 = 480$  seconds. The slopes of the wave on the load up and load release were 1/150 kN/s, 1/75 kN/s, and 1/50 kN/s for the 0.4kN, 0.8kN, and 1.2 kN load levels, respectively. The  
140 0.4kN, 0.8kN, and 1.2 kN cyclic load periods were followed by zero load recovery periods of  $1.25\Delta t_2 = 600$  seconds,  $1.25\Delta t_2 = 600$  seconds, and  $2.5\Delta t_2 = 1200$  seconds, respectively.

At the completion of the cyclic-recovery loading sequences, the specimen was loaded to failure by a monotonic linear ramp. The ramp up to the peak load and unloading were each applied over an interval of  $0.25\Delta t_2 = 120$  seconds.

## 3 Nonlinear time-dependent modeling of S2 columnar freshwater ice

145 The model applied in this section to characterize the nonlinear viscoelastic/viscoplastic response of S2 columnar freshwater ice was presented by Schapery; it was used to model the time-dependent mechanical response of polymers in the nonlinear range under uniaxial stress-strain histories (Schapery, 1969). Schapery's stress-strain constitutive equations are derived from nonlinear thermodynamic principles, and are very similar to the Boltzmann superposition integral form of linear theory (Flügge, 1975). Schapery's model represents the material as a system of an arbitrarily large number of nonlinear springs and dashpots.

150 The equations in this section are presented in terms of load and displacement instead of the original stress-strain relations. The notations of the original equations in (Schapery, 1969) are modified to bring out similarity between all the equations in the paper.

When the applied loads are low enough, the material response is linear. For an arbitrary load input,  $P = P(t)$  applied at  $t = 0$ , Boltzmann's law approximates the load by a sum of a series of constant load inputs and describes the linear viscoelastic  
155 displacement response of the material using the hereditary integral in a single integral constitutive equation. The Boltzmann superposition principle states that the sum of the displacement outputs resulting from each load step is the same as the dis-

placement output resulting from the whole load input. If the number of steps tends to infinity, the total displacement is given as:

$$\delta(t) = C_0 P + \int_0^t \Delta C(t - \tau) \frac{dP}{d\tau} d\tau, \quad (1)$$

160 where  $C_0$  is the initial, time-independent compliance component and  $\Delta C(t)$  is the transient, time-dependent component of compliance.

Turning now to nonlinear viscoelastic response, Schapery developed a simple single-integral constitutive equation from nonlinear thermodynamic theory, with either stresses or strains entering as independent variables (Schapery, 1969). Using load as the independent variable, the displacement response under isothermal and uniaxial loading takes the following form:

$$165 \quad \delta(t) = g_0 C_0 P + g_1 \int_0^t \Delta C(\psi - \psi') \frac{d(g_2 P)}{d\tau} d\tau, \quad (2)$$

where  $C_0$  and  $\Delta C$  are the previously defined components of Boltzmann principle,  $\psi$  and  $\psi'$  are the so-called reduced times defined by:

$$\psi = \int_0^t \frac{dt'}{a_P[P(t')]} \quad \text{and} \quad \psi' = \psi(\tau) = \int_0^\tau \frac{dt'}{a_P[P(t')]} \quad (3)$$

and  $g_0$ ,  $g_1$ ,  $g_2$ , and  $a_P$  are nonlinear functions of the load. Each of these functions represents a different nonlinear influence on the compliance:  $g_0$  models the elastic response,  $g_1$  the transient response,  $g_2$  the loading rate, and  $a_P$  is a time scale shift factor. 170 These load-dependent properties have a thermodynamic origin. Changes in  $g_0$ ,  $g_1$ , and,  $g_2$  reflect third and higher order stress-dependence of the Gibbs free energy, and changes in  $a_P$  are due to similar dependence of both entropy production and the free energy. These functions can also be interpreted as modulus and viscosity factors in a mechanical model representation. In the linear viscoelastic case,  $g_0 = g_1 = g_2 = a_P = 1$ , and Schapery's constitutive equation (2) reduces to Boltzmann's equation (1).

175 Equation (2) contains one time-dependent compliance property, from linear viscoelasticity theory,  $\Delta C$  and four nonlinear load-dependent functions  $g_0$ ,  $g_1$ ,  $g_2$ , and  $a_P$ , which reflect the deviation from the linear viscoelastic response, that need to be evaluated. Schapery's model uses experimental data to evaluate the material property functions in (2). Lou and Schapery outlined a combined graphical and numerical procedure to evaluate these functions (Lou and Schapery, 1971). In their work, a data-reduction method was applied to evaluate the properties from the creep and recovery data. Papanicolaou et al proposed a 180 method capable of analytically evaluating the material functions using only limiting values of the creep-recovery test (Papanicolaou et al., 1999). Numerical methods are also employed and are the most commonly used techniques; they are based on fitting the experimental data to the constitutive equation (LeClair et al., 1999). In the current study, a numerical-experimental procedure is adopted. An optimization procedure is applied using the Nelder-Mead (N-M) method (Nelder and Mead, 1965) to back-calculate the values that achieve the best fit between the model and the experimental data. To avoid multiple fitting

185 treatments of data and account for the mutual dependence of the functions, the properties were determined from the full data. This avoided errors that may result from separating the data into parts and estimating the functions independently from different parts. **This approach of fitting a model with experimental data is common in fracture models with several parameters. Pure experimental methods to determine these parameters has proven extremely difficult and indirect fitting methods have been used instead (Elices et al., 2002).**

190 Schapery later updated his formulation (Schapery, 1997). He added a viscoplastic term to account for the viscoplastic response of the material and stated that the total compliance can be represented as the summation of elastic, viscoelastic, and viscoplastic components. Adamson and Dempsey applied Schapery's updated constitutive equation to model the crack mouth opening displacement of saline ice in an experimental setup similar to the current study (Adamson and Dempsey, 1998). The theory represents the displacement at the crack mouth ( $\delta_{\text{CMOD}}$ ) as the sum of elastic, viscoelastic, and viscoplastic components:

195

$$\delta_{\text{CMOD}} = \delta_{\text{CMOD}}^e + \delta_{\text{CMOD}}^{ve} + \delta_{\text{CMOD}}^{vp} \quad (4)$$

where

$$\delta_{\text{CMOD}}^e = g_0 C_e P \quad (5)$$

200 
$$\delta_{\text{CMOD}}^{ve} = g_1 \int_0^t C_{ve} (\psi - \psi') \frac{d(g_2 P)}{d\tau} d\tau \quad (6)$$

$$\delta_{\text{CMOD}}^{vp} = C_{vp} \int_0^t g_3 P d\tau \quad (7)$$

In the above equations,  $\psi$  and  $\psi'$  are defined in (3).  $g_0, g_1, g_2, g_3$ , and  $a_P$  are nonlinear load functions to be determined. The coefficients  $C_e, C_{ve}$ , and  $C_{vp}$  are the elastic, viscoelastic, and viscoplastic compliances, respectively. Schapery's equation has been developed for uniaxial loading. **The response of the test specimen is dominated by the normal stresses at the direction normal to the X-axis, ahead of the crack (Fig. 1). This stress state can be approximated as uniaxial in the same way as in beam bending; the stress is uniaxial tension at the crack tip and then changes linearly. Thus, Schapery's equations are used to analyze the experimental data.** ~~The experimental problem at hand is not precisely uniaxial, but it is approximated as so, and Schapery's equations are used to analyze the experimental data.~~ Few assumptions are applied at this point and are based on the choices made in (Adamson and Dempsey, 1998). For ice, the elastic displacement is linear with load; this immediately leads to  $g_0 = 1$ . Schapery stated that  $g_1 = a_P = 1$  if the instantaneous jump and drop in the displacement are equal (Schapery, 1969). Examination of the current data shows that this condition is not valid, and the functions need to be evaluated. Accordingly, the following approximations are employed:

210

$$g_1 \propto P^a; \quad g_2 \propto P^{b-1}; \quad g_3 \propto P^{c-1}; \quad a_P \propto P^d \quad (8)$$

215 From Eq. (3):

$$\psi - \psi' = \int_{\tau}^t \frac{dt'}{a_P [P(t')]^d} \quad (9)$$

The viscoelastic compliance is assumed to follow a power law in time with a fractional exponent  $n$ . This gives:

$$C_{ve}(\beta) \approx \kappa \beta^n \quad (10)$$

Incorporating each of these conditions, the total displacement is expressed as

$$220 \quad \delta_{\text{CMOD}} = C_e P + \kappa P^a \int_0^t \left( \int_{\tau}^t \frac{dt'}{[P(t')]^d} \right)^n \frac{d[P(\tau)]^b}{d\tau} d\tau + C_{vp} \int_0^t P^c d\tau \quad (11)$$

where  $\delta_{\text{CMOD}}$ ,  $P$  and  $t$  are in m, N, and seconds, respectively. It follows from (11) that two unknown parameters ( $C_e$ , and  $C_{vp}$ ), one unknown constant ( $\kappa$ ), and five unknown exponents ( $a, b, c, d$ , and  $n$ ) need to be determined. As previously mentioned, the problem is ~~formulated as a least-squares problem and~~ optimized through the N-M technique, by minimizing the objective function  $\mathcal{F}$  given by the difference between the model and data, as shown in (12). The components of the total displacement  
 225 were computed and optimized using MATLAB. **A positive constraint was applied to the model variables.** Initial guesses of the exponents on the load and time functions were assumed based on previous work on saline ice. The optimized values were then obtained by comparing the model response and the experimentally measured response over the full length of the test up to crack growth initiation.

$$\mathcal{F} = \arg \min_{C_e, C_{vp}, a, b, \dots} \sum_{i=1}^N \left\| M_i(C_e, C_{vp}, \kappa, a, b, c, d, n) - D_i \right\|_2 \quad (12)$$

230 where  $M_i$  and  $D_i$  refer to the CMOD values given by the model (11) and the experimental data, respectively.  $\|\cdot\|_2$  is the Euclidean norm of a vector.  $N$  is the number of data points ( $\approx 2e6$  points). **This problem is typically called a least-squares problem when using the Euclidean norm. It is a convex problem because  $\mathcal{F}$  is a convex function and the feasible set is convex. Thus, the optimization algorithm will converge to the global optimal solution.**

As mentioned earlier, Schapery's model originated from the thermodynamic theory. The model is not physically-based, and  
 235 its parameters are not linked to the microstructural properties of the ice (dislocation density, grain size, ...). In addition, the analysis does not account for the formation of fracture process zone in the vicinity of the crack tip. Schapery's formulation models the experimental response until crack growth initiation and does not account for crack propagation.

#### 4 Experimental and modelling ~~R~~results and discussions

This section presents the results measured and computed for the LC tests. The current results are compared with the fracture  
 240 results of monotonically loaded DC tests of the same ice and same specimen size (3m x 6m) (Gharamti et al., 2021). The main



aim is to elucidate the effect of creep and cyclic sequences on the fracture properties.

## 4.2 Effect of the creep and cyclic sequences on the fracture properties

Table 1 shows the measured and computed parameters for the LC experiments.  $P_{\max}$  is the measured peak load which is also  
245 the failure load.  $t_f$  represents the time to failure, computed from the fracture ramp. ~~From the failure load and dimensions, an~~  
~~apparent fracture toughness ( $K_Q$ ) is computed using the weight function procedure outlined in Section 4 of (Gharamti et al.,~~  
2021). CMOD is ~~computed~~ measured at crack growth initiation. CMOD indicates the displacement rate at the crack mouth and  
is obtained by dividing CMOD by the failure time. Similarly, NCOD1 (see Fig. 1) represents the displacement at crack growth  
initiation near the initially sharpened crack tip. NCOD1 indicates the displacement rate in the vicinity of the tip and is obtained  
250 by dividing NCOD1 by the failure time.

Fig. 4 gives the results of the ~~apparent fracture toughness  $K_Q$~~  peak load  $P_{\max}$ , crack mouth opening displacement CMOD,  
and near crack-tip opening displacement NCOD1 as a function of the loading ~~rate~~ time for the DC tests (Gharamti et al., 2021)  
and the current LC tests. In these subplots, first-order power-law fits were applied to the data of the DC tests. The LC values  
lie above, below, and along the DC fit. No clear effect of creep and cyclic loading on the fracture properties was detected.

255 Figs. 5a and 5b show the experimental load versus the crack opening displacement at the crack mouth for the DC and the  
LC tests, respectively. Fig. 5c displays a zoomed view of the fracture ramp of the LC tests. Comparing the failure loads of  
the DC and LC tests indicates that the failure loads, of tests with comparable loading rates, were similar. Therefore, in these  
experiments, the creep and cyclic sequences had no influence on the failure load.

Table 1 presents several elastic moduli for each test. The elastic moduli were calculated from the load-CMOD record fol-  
260 lowing Section 4 of (Gharamti et al., 2021). For the creep tests (RP15 and RP16), this procedure is repeated for the four creep  
cycles, resulting in  $E_1$ ,  $E_2$ ,  $E_3$ ,  $E_4$ , and for the fracture ramp, resulting in  $E_f$ . Similarly for the cyclic tests (RP17, RP18,  
and RP19), the moduli calculation was done for the last cycle of each cyclic sequence, giving steady state moduli  $E_1$ ,  $E_2$ ,  $E_3$ ,  
and for the fracture ramp, resulting in  $E_f$ . Some of the values are missing, caused by the fact that the initial portion of the  
associated load-CMOD curve was very noisy. The values of the elastic moduli calculation for the creep/cyclic sequences and  
265 fracture ramps were similarly linear upon load application, as shown by the loading slope in Figs. 5c, 6a, and 6b. This linearity  
justifies the choice of  $g_0 = 1$  in the elastic CMOD component in Eq. (5).

Table 1 in (Gharamti et al., 2021) presents the elastic modulus ( $E_{\text{CMOD}}$ ) calculated at the crack mouth for the DC tests;  
 $E_{\text{CMOD}}$  is similar to  $E_f$  in Table 1 here; both values lie within the same range. Therefore, the creep and cyclic sequences  
preceding the fracture ramp did not affect the load-CMOD prepeak behavior. However, the sequences affected the post-peak  
270 response as can be distinguished from Fig. 5b which displays ~~more a longer~~ decay behavior than Fig. 5a. The gradual decay of  
the load portrays the time dependency in the behavior of freshwater ice.

## 4.3 Ice response under the testing conditions

Fig. 7 shows the experimental results for RP16: the applied load and the crack opening displacements at the crack mouth (CMOD), halfway of the crack (COD), and 10 cm behind the tip (NCOD1) (see Fig. 1). Similarly, Fig. 8 shows the experimental response for RP17. The time-dependent nature of the ice response is evident. A complete load-CMOD curve was obtained during loading and unloading for each test of Table 1, indicating stable crack growth.

It is clear from Figs. 7b and 8b that the CMOD, COD, and NCOD1 displacements were composed mainly of elastic and viscoplastic components. No **significant** viscoelasticity was detected in the displacement-time records for all the tests. The primary (transient) creep stage was **almost absent or instantaneous**. The load sequences were characterized by a non-decreasing displacement rate at all levels. The displacement-time slope was linear and constant, indicating that the secondary/steady-state creep regime dominated during each load application. Although the recovery time was longer than the loading time,  $\geq 1.25\Delta t_1$  (Creep test, Fig. 3a and Section 2.2) and  $\geq 1.25\Delta t_2$  (Cyclic test, Fig. 3b and Section 2.3), the recovery (unload) phases consisted mainly of an elastic recovery (instantaneous drop) and unrecovered viscoplastic displacement. The behavior as observed resembles the response of a **simple** Maxwell model composed of a series combination of a nonlinear spring and nonlinear dashpot. There is no delayed elastic recovery, but there is the elastic response and a permanent deformation.

Figs. 6a and 6b support the same analysis. Unlike the viscoelastic response (Fig. 6c) which displays no residual displacement in the loading and unloading hysteresis diagram, the current load-CMOD plots showed large permanent displacement after each loading cycle. **This concludes that the response of columnar freshwater S2 ice in these tests was overall elastic-viscoplastic.**

~~Interestingly, the ice behavior in the current study differs from previous experimental creep and cyclic work on freshwater ice. Large delayed elastic or recoverable component has been previously observed. Several researchers performed creep experiments at lower temperatures (Mellor and Cole, 1981, 1982, 1983; Cole, 1990; Duval et al., 1991) and reported considerable recovery. Duval conducted torsion creep tests on glacier ice at a similar testing temperature of  $-1.5\text{ C}$  (Duval, 1978). When unloaded, the ice exhibited creep recovery. According to his analysis: during loading, the internal stresses opposing the dislocation motion increases; upon unloading, the movement of dislocations produced the reversible deformation and is caused by the relaxation of internal stresses. Sinha (Sinha, 1978, 1979) concluded that high-temperature creep of polycrystalline ice is associated with grain boundary sliding. Cole developed a physically-based constitutive model in terms of dislocation mechanics (Cole, 1995) and quantified two mechanisms of anelasticity: dislocation and grain boundary relaxations. He demonstrated that the increased temperature sensitivity of the creep properties of ice within a few degrees of the melting point is due to a thermally induced increase in the dislocation density (Cole, 2020). The question then arises as to why columnar freshwater ice tested at  $-2\text{ C}$  did not show a delayed elastic effect, and the microstructural changes were mainly irreversible upon unloading?~~

~~An influencing factor is the mechanisms taking place in the process zone. There is possibility that the loading conditions produced dislocations which would ordinarily generate some viscoelastic deformation upon unloading. However, local damage in the process zone relieved the internal stresses that are needed to drive the dislocation recovery. Thus, any microstructural damage that occurred during loading manifested as permanent deformation at the end of the test. It is noteworthy that the earlier studies used test sizes which are smaller than the plate size used here. It was shown in the DC fracture tests (Gharamti et al., 2021) that scale had an effect at the tested loading rates. It is probable that the specimen size influenced the time-dependent~~

deformation of freshwater ice. When the specimen dimensions are several meters, apparently viscoelasticity is not an important deformation component.

310 ~~The ice response indicates that the combined effects of the geometry, the applied loading profiles, the warm temperature (-2 C), and the testing conditions triggered an instantaneous transformation from the primary stage to the steady-state stage, resulting in permanent irreversible deformation that accumulated after each creep/cyclic-recovery sequence. This concludes that the response of columnar freshwater S2 ice in these tests is elastic-viscoplastic.~~

#### 4.4 Schapery-optimization **Nonlinear** modelling analysis

The nonlinear theory, outlined in Section 3, was used to analyze the experiments. The results of the initial optimization trials 315 confirmed the previous analysis; the viscoelastic component  $\delta_{\text{CMOD}}^{\text{ve}}$  had no effect on the final fit between the data and the model. The variation of the constants corresponding to  $\delta_{\text{CMOD}}^{\text{ve}}$ ,  $\kappa$ ,  $a$ ,  $b$ ,  $d$ , and,  $n$  didn't affect the final converged values of  $C_e$ ,  $C_{vp}$ , and  $c$ .

The final optimization runs were carried out by considering the elastic and viscoplastic components (first and last terms of Eq. (11)) only. This resulted in 2 parameters,  $C_e$  and  $C_{vp}$ , and one exponent  $c$ , that need to be optimized. The optimization 320 converged results are given in Table 2:  $C_e$ ,  $C_{vp}$  and  $c$ . For all the tests, the %reduction of the objective function exceeded 95% and about 110 iterations were needed to reach convergence. A value of  $c = 1$  for the viscoplastic load function provided the best fit between the model and the experiment at all load levels over the total experimental time up to the peak load. The final compliance values of the elastic and viscoplastic components were in the ranges  $1.8\text{-}3.8 \times 10^{-8} \text{mN}^{-1}$  and  $0.2\text{-}1 \times 10^{-10} \text{mN}^{-1} \text{s}^{-1}$ , respectively.

325 Figs. 9 and 10 give the model results, obtained using Eqs. (4-10), and the experimental results for experiments RP16 and RP17, respectively. Figs. 9a and 9b show the measured load and the load applied to the model and the measured CMOD-time record compared to the response of the model, respectively for RP16. Figure 10 shows similar plots for experiment RP17. Test RP17 showed an excellent model-experiment fit for the three cyclic-recovery sequences over the load and unload periods. The recovery displacements were fitted accurately by the model in the three recovery periods. The experimental response for the 330 creep-recovery test RP16 appeared to conform to the model results, but the model underestimated the recovery displacement in the first two cycles with a maximum misfit of  $\approx 2e^{-5} \mu\text{m}$ . Schapery's model has been tested for creep-recovery sequences of saline ice with an increasing load profile (Schapery, 1997; Adamson and Dempsey, 1998; LeClair et al., 1999, 1996). This is the first application of the model with a load profile of increasing and decreasing load levels (Fig. 3a). The model succeeded to follow the increasing and decreasing load levels and the corresponding recovery phases. The model generated the peak 335 displacement values for all load levels with a misfit of  $1e^{-5} \mu\text{m}$  for the last two creep cycles. The observed misfit ( $1\text{-}2 e^{-5} \mu\text{m}$ ) is small and should be ignored. It is related to the accuracy of the measurement line (LVDT + amplifier + data processing unit) which is affected by many environmental and technical factors. Thus, the implemented model provided a good fit with the data over the creep-recovery and cyclic-recovery sequences.

340 Considering the fracture ramp, Schapery's nonlinear equation succeeded to model the monotonic displacement response up to crack growth initiation perfectly well for all the tests. As previously mentioned, the model does not account for crack

propagation, so modeling was applied until the peak load. The model was also successful in predicting the critical crack opening displacement values at the failure load. Thus, the model gives a very close prediction of the experimental data over the whole loading profile up to the failure load. The other tests displayed the same experiment-model agreement.

345 In this study, Schapery's constitutive model is tested for the first time for freshwater ice. The match between the model and the measured data, over the creep/cyclic-recovery sequences and fracture monotonic ramp, provides a firm support of the ability of Schapery's constitutive model to describe the time-dependent response of columnar freshwater S2 ice up to crack growth initiation. Figs. 11a and 11b show the contribution of each individual model component, elastic and viscoplastic, to the total CMOD displacement, for RP16 and RP17, respectively. As mentioned earlier, the elastic and viscoplastic components account for the total deformation. For RP16, the viscoplastic component dominated over the elastic component. For RP17, the  
350 elastic and viscoplastic components contributed equally to the total displacement.

The applicability of the proposed model and the fitted parameters are limited to the studied ice type, geometry, specimen size, ice temperature, and the current testing conditions. Variation in the operating conditions will change the dominant deformation mechanisms and the ice behavior; and accordingly, new model parameters are needed to adapt to the new response.

## 5 Discussion

355 Interestingly, the ice behavior in the current study differs from previous experimental creep and cyclic work on freshwater ice. Large delayed elastic or recoverable component has been previously observed. Several researchers performed creep experiments on granular freshwater ice at lower temperatures (Mellor and Cole, 1981, 1982, 1983; Cole, 1990; Duval et al., 1991) and reported considerable recovery. Duval conducted torsion creep tests on glacier ice at a similar testing temperature of -1.5 C (Duval, 1978). When unloaded, the ice exhibited creep recovery. According to his analysis: during loading, the internal stresses  
360 opposing the dislocation motion increases; upon unloading, the movement of dislocations produced the reversible deformation and is caused by the relaxation of internal stresses. Sinha (1978, 1979) studied columnar-grained freshwater ice and concluded that the high-temperature creep is associated with grain boundary sliding. Cole developed a physically-based constitutive model in terms of dislocation mechanics (Cole, 1995) and quantified two mechanisms of anelasticity: dislocation and grain boundary relaxations. He demonstrated that the increased temperature sensitivity of the creep properties of ice within a few degrees of  
365 the melting point is due to a thermally induced increase in the dislocation density (Cole, 2020). The question then arises as to why warm columnar freshwater ice tested here showed no significant delayed elastic effect, and the microstructural changes were mainly irreversible upon unloading?

Knauss presented a thorough review of the time-dependent fracture models available to date (Knauss, 2015). The essence of the models is based on modelling the behavior in a finite cohesive/process zone which is attached to the traction-free crack  
370 tip. The one-parameter fracture mechanics encompassed by the apparent fracture toughness is not applicable (Dempsey et al., 2018). It is believed that the mechanisms taking place in the process zone play an influencing role in the current tests. There is possibility that the loading conditions produced dislocations which would ordinarily generate some viscoelastic deformation upon unloading. However, following Duval analysis of internal stresses, the nonlinear fracture mechanisms in the process zone

relieved the internal stresses that are needed to drive the dislocation recovery. Thus, any microstructural damage that occurred during loading manifested as permanent deformation at the end of the test.

Sinha (1979) developed a nonlinear viscoelastic model, incorporating the grain size effect, to describe the high-temperature creep of polycrystalline materials. Delayed elastic strain was shown to exhibit an inverse proportionality with grain size. This grain size effect was attributed to the increasing contributions of grain boundary sliding and accordingly the contribution of the delayed elastic component to the total deformation. The same behavior is observed in metals. This suggests that the grain size of the ice samples (3-10 mm, Fig. 2b) in this study was coarse enough not to produce any measurable viscoelastic deformation under the testing conditions.

It is noteworthy that the earlier studies used test sizes which are smaller than the plate size used here. It was shown in the DC fracture tests (Gharamti et al., 2021) that scale had an effect at the tested loading rates. It is probable that the specimen size influenced the time-dependent deformation of freshwater ice. The current tests suggest that for the large sample size and the kind of ice studied (very warm freshwater ice) under the loading applied, viscoelasticity is not an important deformation component. The experimental results support this prediction, but more tests are needed to make more general conclusions.

Overall, the ice response indicates that the combined effects of the geometry, the microstructure, the applied loading profiles and the warm temperature triggered an instantaneous transformation from the primary stage to the steady-state stage, resulting in an elastic-viscoplastic response and a permanent irreversible deformation that accumulated after each creep/cyclic-recovery sequence.

## 6 Conclusions

In the present work, five 3m x 6m warm freshwater S2 ice specimens were tested under creep/cyclic-recovery sequences followed by a monotonic ramp at -2°C. The temperature at the top surface was about -0.3°C. The tests were load controlled and led to complete fracture of the specimen. The purpose of this study was to examine the time-dependent behavior of freshwater ice using a joint experimental-modeling approach.

In the experimental part, the tests aimed to (1) measure and examine the time-dependent response of columnar freshwater S2 ice through the applied creep/cyclic-recovery sequences and (2) investigate the effect of creep and cyclic sequences on the fracture parameters/behavior through the fracture monotonic ramp. The current tests were compared with other monotonically loaded tests of the same ice, and fracture parameters were computed and analyzed. The results showed that the creep and cyclic sequences had no clear effect on the apparent fracture toughness, the failure load, and the crack opening displacements at crack growth initiation. The ice response at the testing conditions was overall elastic-viscoplastic, and the steady-state regime dominated the loading phases. The loading phases displayed an instantaneous transformation from the primary (transient) stage to the steady-state regime, which resulted in permanent (unrecoverable) displacement. The conducted experiments provided a novel observation for the time-dependent behavior of freshwater ice. Though the delayed elastic component has been reported as a major creep component in freshwater ice, no significant viscoelasticity was detected in this study. The primary (transient) creep stage was absent. This indicates that the collective effects of several factors were discussed as possibly contributing

to the observed behavior: the very warm columnar freshwater ice, large sample size, coarse grain size, and applied loading. the testing conditions and plate configuration triggered an instantaneous transformation to the steady-state regime resulting in permanent (unrecoverable) displacement.

410 In the modeling part, Schapery's nonlinear constitutive model was applied for the displacement response at the crack mouth. The elastic-viscoplastic formulation succeeded to predict the experimental response of columnar freshwater S2 ice over the applied loading profile up to crack growth initiation. The model parameters were obtained via an optimization procedure using the N-M method by comparing the model and experimental CMOD values.

415 The proposed model parameters are valid only for the studied ice type, geometry, specimen size, ice temperature, and the range of applied load experienced in the experiments. Schapery's model was selected in this study, as it is able to capture the sort of time dependent behavior known to occur in ice and produces a simple and expedient way to help understand the observed behavior. More thorough analysis with a physically-based approach is left to the future.

*Code and data availability.* The code used for material modeling is written in Matlab. Scripts used for analysis and more detailed information of the experimental results are available from the authors upon request.

420 *Author contributions.* All authors designed the study and performed the experiments. I.E.G. generated the results and drafted the paper. All authors commented on the text.

*Competing interests.* The authors declare that they have no conflict of interest.

425 *Acknowledgements.* This work was funded through the Finland Distinguished Professor programme "Scaling of Ice Strength: Measurements and Modeling", and through the ARAJÄÄ research project, both funded by Business Finland and the industrial partners Aker Arctic Technology, Arctech Helsinki Shipyard, Arctia Shipping, ABB Marine, Finnish Transport Agency, Suomen Hyötytuuli Oy, and Ponvia Oy. This financial support is gratefully acknowledged. The authors would like to thank Dr. David Cole for taking the time and effort to review the manuscript. The first author (I.E.G.) is thankful to Dr. Kari Santaoja for useful and enlightening discussions. The second author (J.P.D.) thanks Business Finland for support by the FiDiPro Professorship from Aalto University, and the sabbatical support from Aalto University, which collectively supported an annual visit 2015-2016, and summer visits 2017-2019.

## 430 References

- Abdel-Tawab, K. and Rodin, G. J.: Analysis of primary creep of S2 fresh-water and saline ice, *Cold Regions Science and Technology*, 26, 83–96, 1997.
- Adamson, R. M. and Dempsey, J. P.: Field-scale in-situ compliance of arctic first-year sea ice, *Journal of Cold Regions Engineering*, 12, 52–63, 1998.
- 435 Ashby, M. F. and Duval, P.: The creep of polycrystalline ice, *Cold Regions Science and Technology*, 11, 285–300, 1985.
- Ashton, G. D.: *River and lake ice engineering*, Water Resources Publication, Littleton, Colorado, 1986.
- Cole, D.: On the physical basis for the creep of ice: the high temperature regime, *Journal of Glaciology*, 66, 401–414, 2020.
- Cole, D. M.: Reversed direct-stress testing of ice: Initial experimental results and analysis, *Cold Regions Science and Technology*, 18, 303–321, 1990.
- 440 Cole, D. M.: A model for the anelastic straining of saline ice subjected to cyclic loading, *Philosophical Magazine A*, 72, 231–248, 1995.
- Dempsey, J. P., Cole, D. M., and Wang, S.: Tensile fracture of a single crack in first-year sea ice, *Philosophical Transactions of the Royal Society A*, 376, 20170346, 2018.
- Duval, P.: Anelastic behaviour of polycrystalline ice, *Journal of Glaciology*, 21, 621–628, 1978.
- Duval, P., Kalifa, P., and Meyssonier, J.: Creep constitutive equations for polycrystalline ice and effect of microcracking, in: *International Union on Theoretical and Applied Mechanics (IUTAM)*, pp. 55–67, 1991.
- 445 Elices, M., Guinea, G. V., Gomez, J., and Planas, J.: The cohesive zone model: advantages, limitations and challenges, *Engineering Fracture Mechanics*, 69, 137–163, 2002.
- Flügge, W.: *Viscoelasticity*. Springer-Verlag, Berlin, 1975.
- Gharamti, I. E., Dempsey, J. P., Polojärvi, A., and Tuhkuri, J.: Fracture of S2 columnar freshwater ice: size and rate effects, *Acta Materialia*, 202, 22–34, 2021.
- 450 Iliescu, D. and Schulson, E.: Brittle compressive failure of ice: monotonic versus cyclic loading, *Acta materialia*, 50, 2163–2172, 2002.
- Iliescu, D., Murdza, A., Schulson, E. M., and Renshaw, C. E.: Strengthening ice through cyclic loading, *Journal of Glaciology*, 63, 663–669, 2017.
- Jellinek, H. and Brill, R.: Viscoelastic properties of ice, *Journal of Applied Physics*, 27, 1198–1209, 1956.
- 455 Jorgen, V. G. and Picu, B. C.: Effect of step-loading history and related grain-boundary fatigue in freshwater columnar ice in the brittle deformation regime, *Philosophical magazine letters*, 77, 241–247, 1998.
- Knauss, W. G.: A review of fracture in viscoelastic materials, *International Journal of Fracture*, 196, 99–146, 2015.
- Le Gac, H. and Duval, P.: Constitutive relations for the non elastic deformation of polycrystalline ice, in: *Physics and Mechanics of Ice*, pp. 51–59, 1980.
- 460 LeClair, E. S., Schapery, R. A., and Dempsey, J. P.: Tensile creep of saline ice, in: *Symposium on Inelasticity and Damage in Solids Subject to Microstructural Change*, pp. 143–153, St. John's, Newfoundland, Canada, 1996.
- LeClair, E. S., Schapery, R. A., and Dempsey, J. P.: A broad-spectrum constitutive modeling technique applied to saline ice, *International Journal of Fracture*, 97, 209–226, 1999.
- Lou, Y. C. and Schapery, R. A.: Viscoelastic characterization of a nonlinear fiber-reinforced plastic, *Journal of Composite Materials*, 5, 208–234, 1971.
- 465 Mellor, M. and Cole, D.: Cyclic loading and fatigue in ice, *Cold regions science and technology*, 4, 41–53, 1981.

- Mellor, M. and Cole, D. M.: Deformation and failure of ice under constant stress or constant strain-rate, *Cold Regions Science and Technology*, 5, 201–219, 1982.
- Mellor, M. and Cole, D. M.: Stress/strain/time relations for ice under uniaxial compression, *Cold Regions Science and Technology*, 6, 207–  
470 230, 1983.
- Michel, B.: A mechanical model of creep of polycrystalline ice, *Canadian Geotechnical Journal*, 15, 155–170, 1978.
- Murdza, A., Schulson, E. M., and Renshaw, C. E.: Strengthening of columnar-grained freshwater ice through cyclic flexural loading, *Journal of Glaciology*, pp. 1–11, 2020.
- Nelder, J. A. and Mead, R.: A simplex method for function minimization, *The Computer Journal*, 7, 308–313, 1965.
- 475 Palmer, A. C., Goodman, D. J., Ashby, M. F., Evans, A. G., Hutchinson, J. W., and Ponter, A. R. S.: Fracture and its role in determining ice forces on offshore structures, *Annals of Glaciology*, 4, 216–221, 1983.
- Papanicolaou, G., Zaoutos, S., and Cardon, A.: Further development of a data reduction method for the nonlinear viscoelastic characterization of FRPs, *Composites Part A: Applied Science and Manufacturing*, 30, 839–848, 1999.
- Santaoja, K.: Ph.D. Thesis: Mathematical modelling of deformation mechanisms in ice, Technical Research Center of Finland, Espoo, 1990.
- 480 Schapery, R.: Thermoviscoelastic constitutive equations for polycrystalline ice, *Journal of Cold Regions Engineering*, 11, 146–157, 1997.
- Schapery, R. A.: On the characterization of nonlinear viscoelastic materials, *Polymer Engineering & Science*, 9, 295–310, 1969.
- Sinha, N. K.: Rheology of columnar-grained ice, *Experimental Mechanics*, 18, 464–470, 1978.
- Sinha, N. K.: Grain boundary sliding in polycrystalline materials, *Philosophical Magazine A*, 40, 825–842, 1979.
- Sunder, S. S. and Wu, M. S.: A differential flow model for polycrystalline ice, *Cold Regions Science and Technology*, 16, 45–62, 1989.
- 485 Sunder, S. S. and Wu, M. S.: On the constitutive modeling of transient creep in polycrystalline ice, *Cold Regions Science and Technology*, 18, 267–294, 1990.



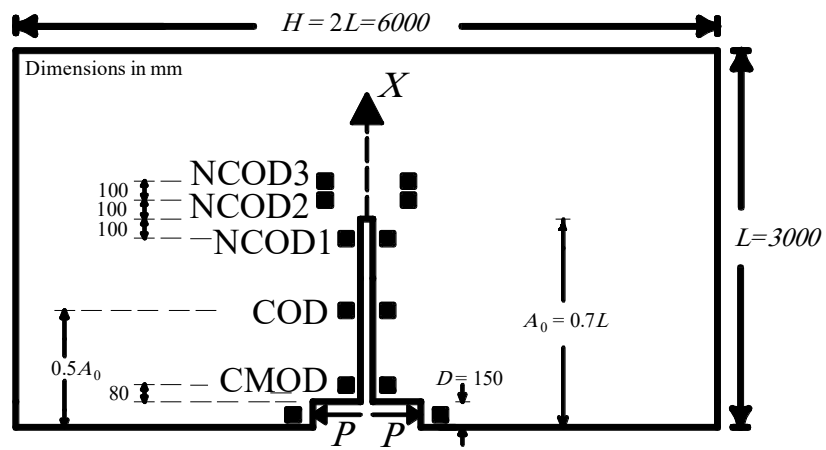
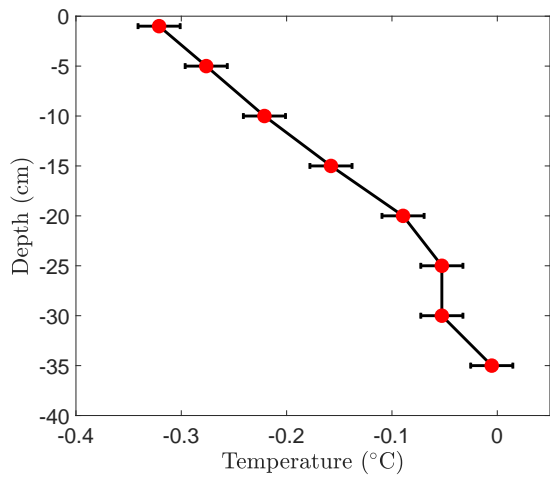
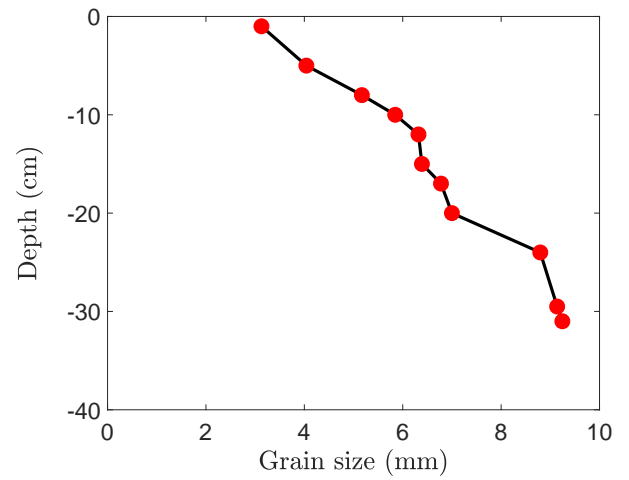


**Figure 1.** (a) Specimen geometry, edge cracked rectangular plate of length  $L$ , width  $H$ , and crack length  $A_0$ .

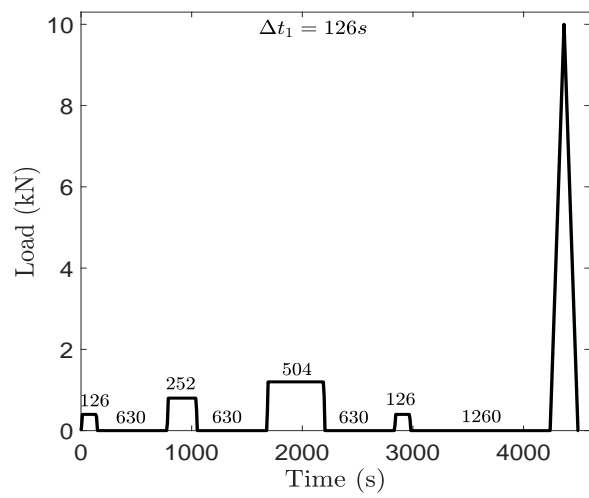


(a)

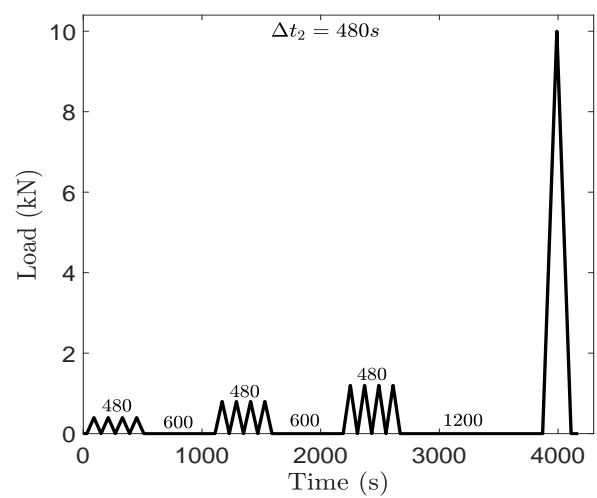


(b)

**Figure 2.** (a) Temperature profile. Each data point represents the average of measurements taken at the same depth of different ice cores throughout the one month duration of the test program. (b) Grain size distribution. Each data point is measured from one thin section.



(a)



(b)

**Figure 3.** Loading consisting of (a) creep-recovery and (b) cyclic sequences followed by a monotonic fracture ramp. The number above each segment indicates the duration in s.

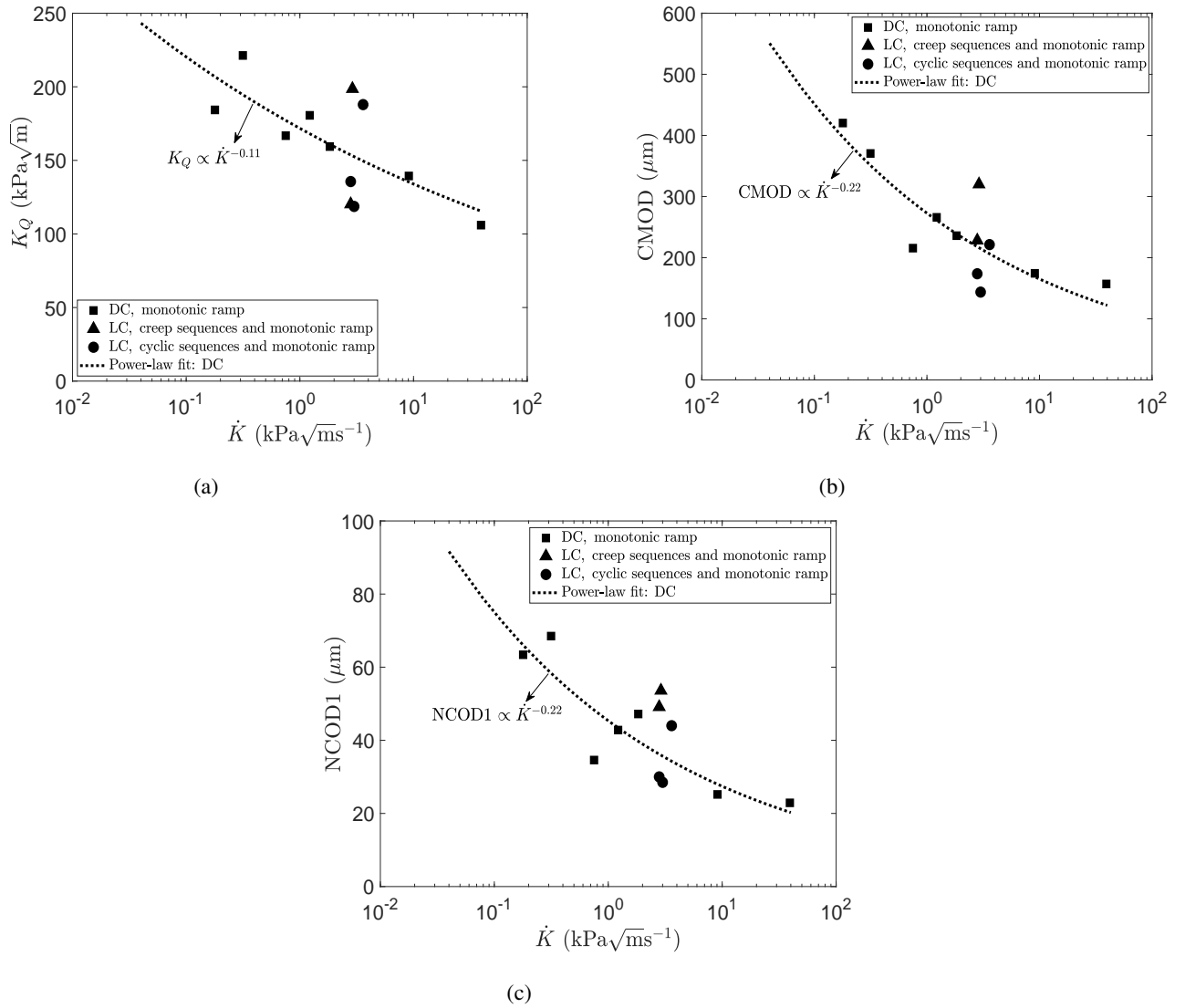


**Figure 4.** Experimental results for the (a) apparent fracture toughness  $K_Q$ , (b) crack mouth opening displacement CMOD and (c) near crack-tip opening displacement NCOD1 at crack growth initiation, as a function of loading rate for the monotonically-loaded DC tests (Gharanti et al., 2021) and the creep/cyclic and monotonically-loaded LC tests.

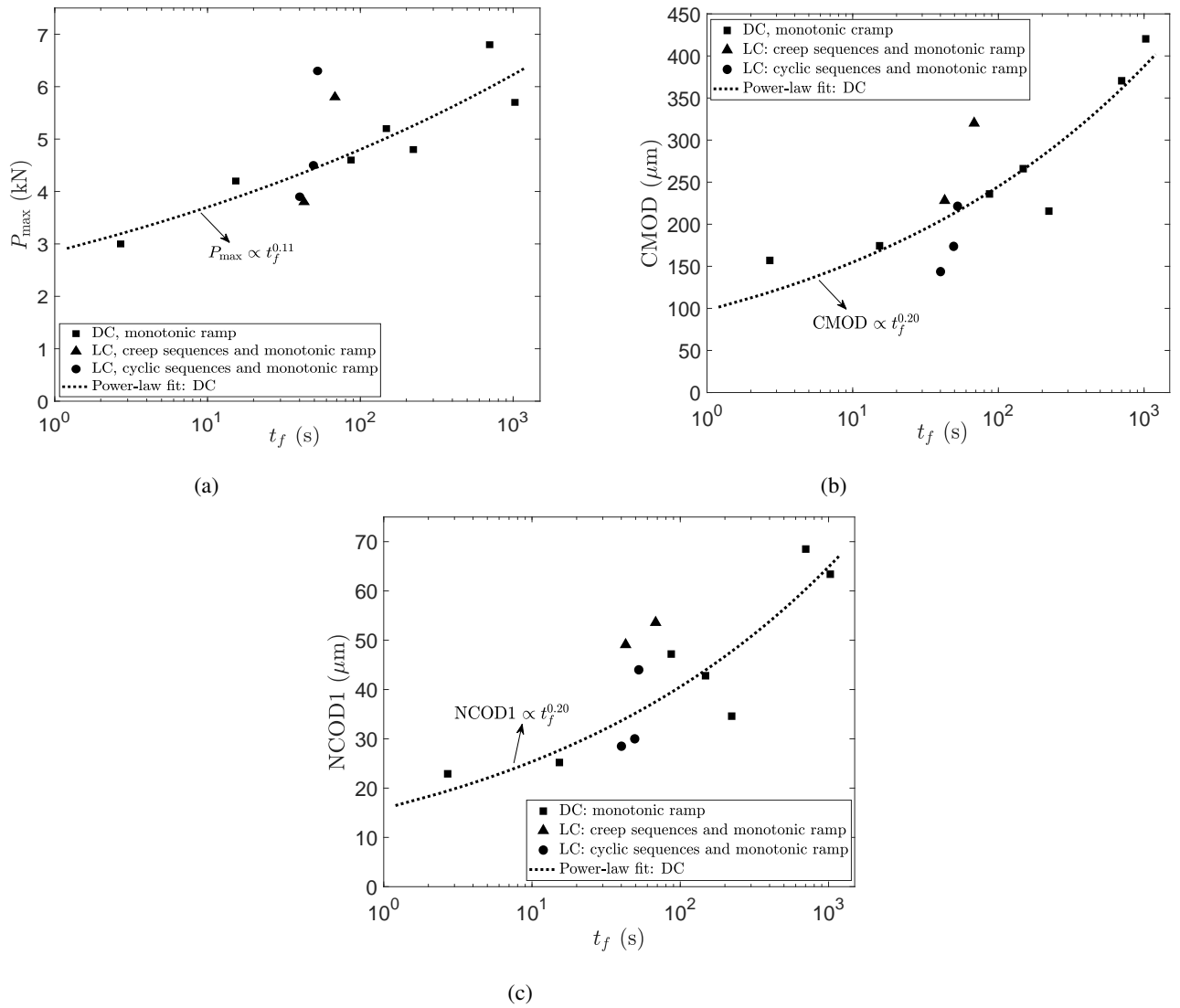


**Figure 4.** Experimental results for the (a) peak load  $P_{\max}$ , (b) crack mouth opening displacement CMOD and (c) near crack tip opening displacement NCOD1 at crack growth initiation, as a function of time to failure  $t_f$  for the monotonically-loaded DC tests (Gharamti et al., 2021) and the creep/cyclic and monotonically-loaded LC tests.

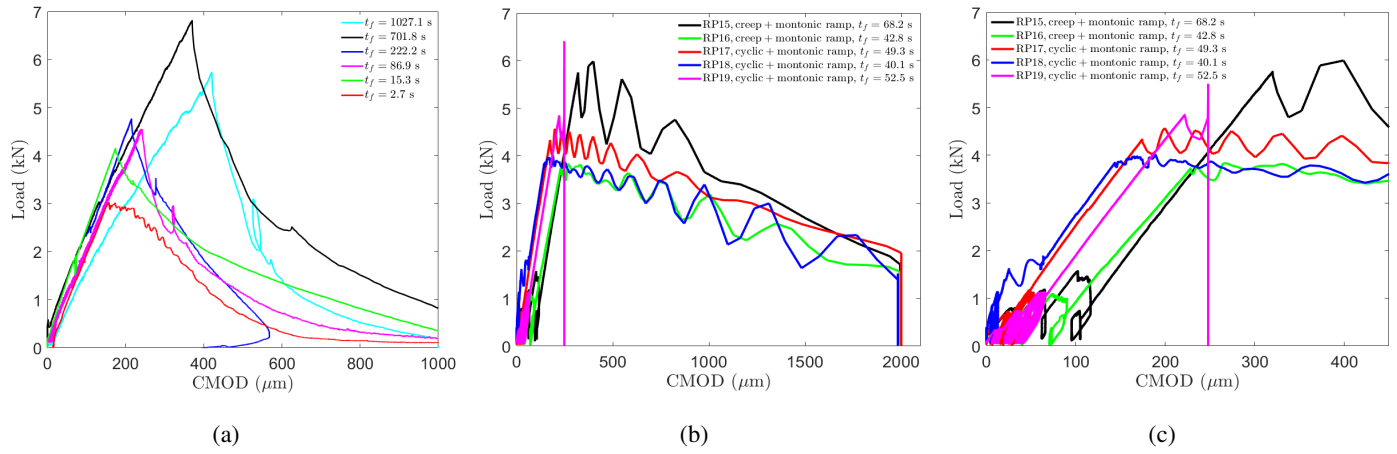


**Figure 5.** Measured load versus CMOD for the (a) DC tests Gharamti et al. (2021), (b) LC tests, and (c) LC tests up to the peak load.

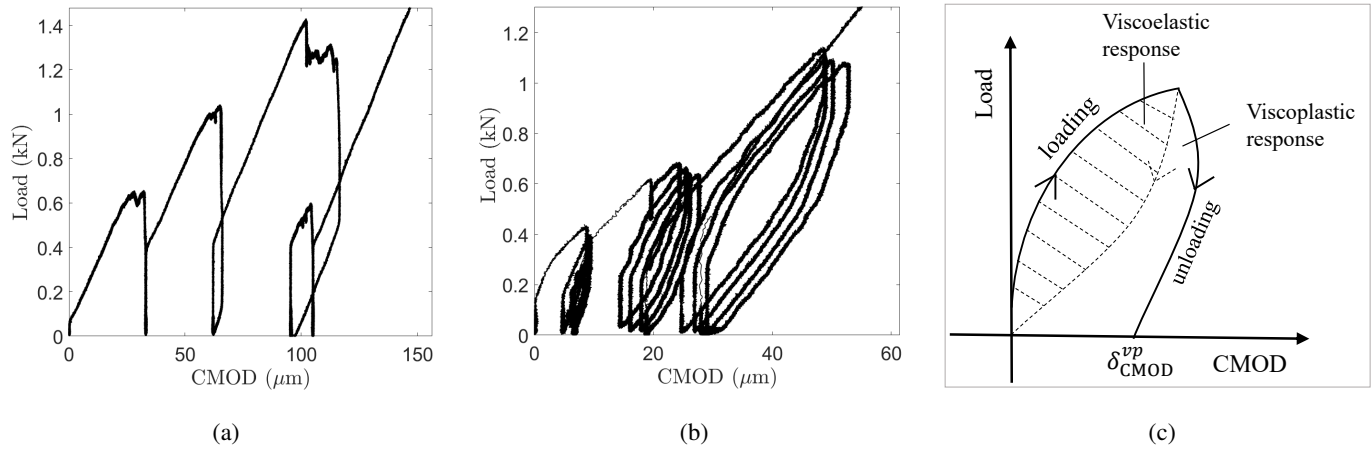


**Figure 6.** Load versus CMOD over the (a) creep-recovery cycles for RP15 and the (b) cyclic-recovery sequences for RP17. (c) Schematic illustration of the hysteresis load-displacement diagram. The whole of the hysteresis loop area is the energy loss per cycle. The dashed area is the part of that total that is due to the viscoelastic mechanism and the rest is due to viscous processes.

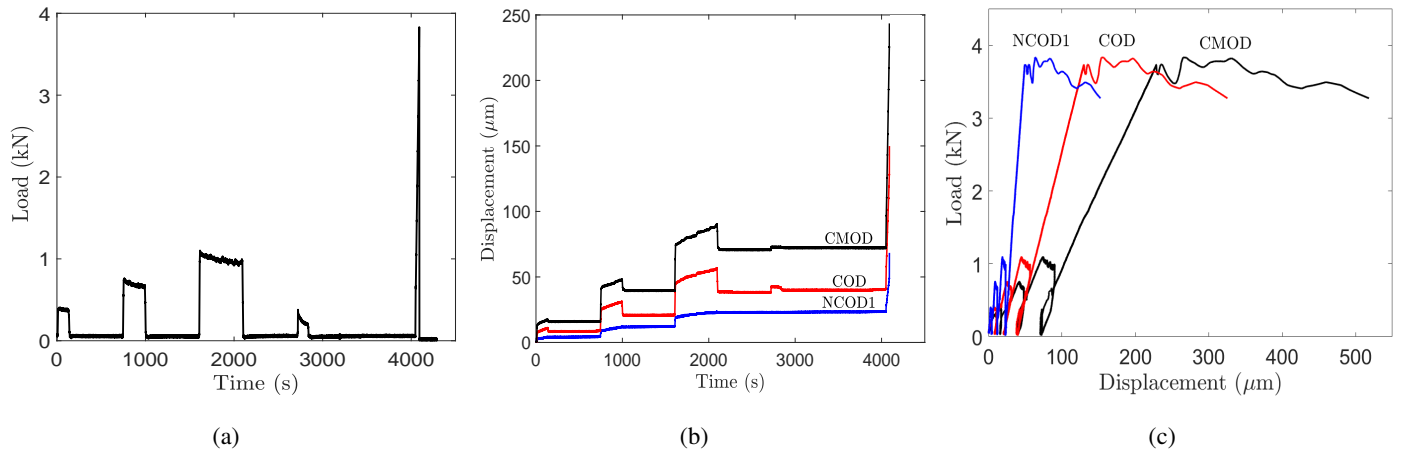


**Figure 7.** Experimental results for RP16. (a) Load at the crack mouth, see Fig. 1. (b) Displacement - time records. (c) Load - displacement record.



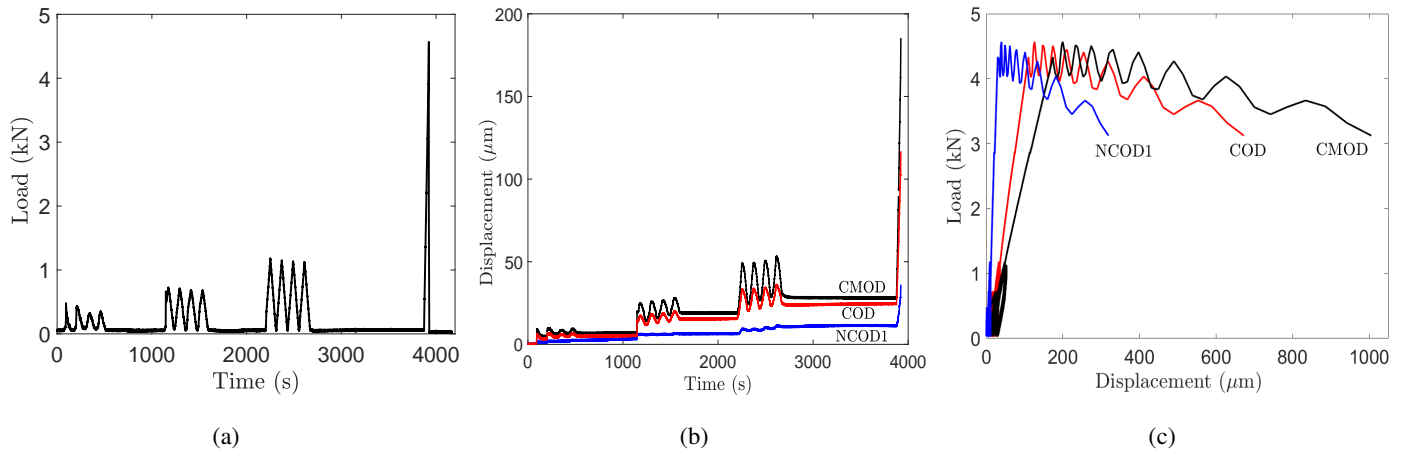
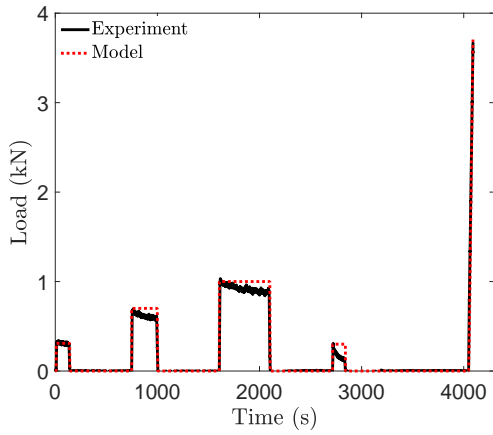
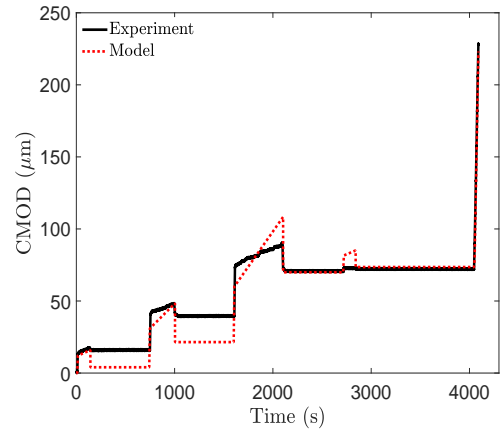


**Figure 8.** Experimental results for RP17. (a) Load at the crack mouth, see Fig. 1. (b) Displacement - time records. (c) Load - displacement record.

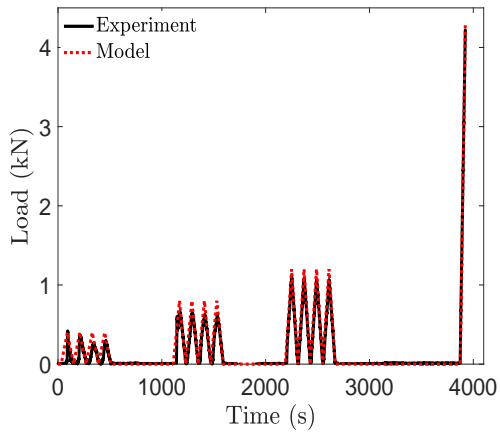


(a)

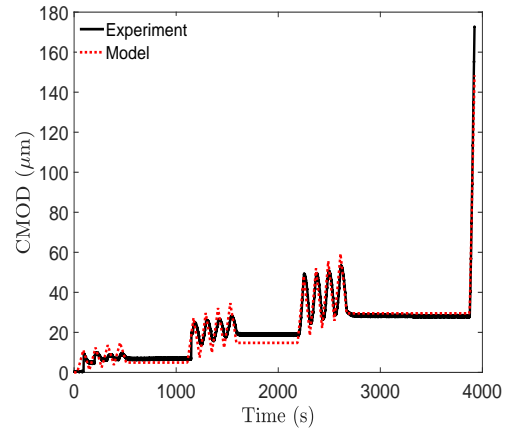


(b)

**Figure 9.** Experimental and model results for RP16. (a) Load at the crack mouth, see Fig. 1. (b) CMOD - time records

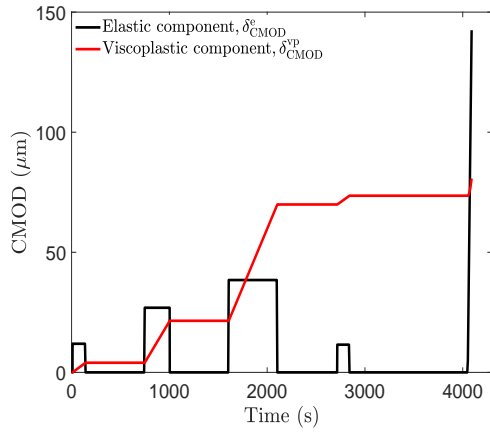


(a)

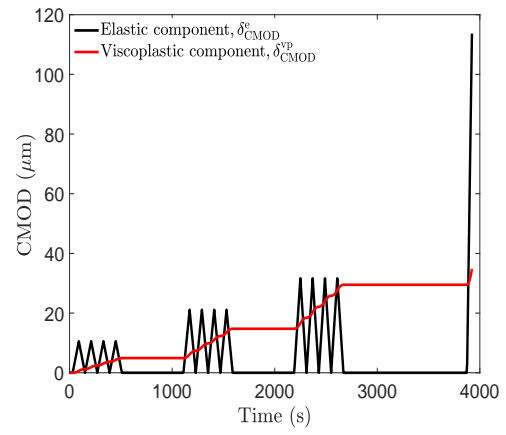


(b)

**Figure 10.** Experimental and model results for RP17. (a) Load at the crack mouth, see Fig. 1. (b) CMOD - time records



(a)



(b)

**Figure 11.** Contribution of each individual model component to the total CMOD displacement for (a) RP16 and (b) RP17.

**Table 1.** Measured experimental data and computed results for the LC tests.

Test	Type	$L$	$H$	$A_0$	$h$	$E_1$	$E_2$	$E_3$	$E_4$	$E_f$	$P_{\max}$	$t_f$	$K_Q$	$\dot{K}$	CMOD	CM $\dot{O}D$	NCOD1	NC $\dot{O}D1$
		(m)	(m)	(m)	(mm)	(GPa)	(GPa)	(GPa)	(GPa)	(GPa)	(kN)	(s)	( $\text{kPa}\sqrt{\text{m}}$ )	( $\text{kPa}\sqrt{\text{ms}}^{-1}$ )	( $\mu\text{m}$ )	( $\mu\text{ms}^{-1}$ )	( $\mu\text{m}$ )	( $\mu\text{ms}^{-1}$ )
RP15	creep	3	6	2.1	364	6.6	6.7	7.3	7.4	6.9	5.8	68.2	<del>198.6</del>	<del>2.9</del>	320.1	4.7	53.6	0.8
RP16	creep	3	6	2.1	385	5.6	5.8	7.6	-	6.0	3.8	42.8	<del>120.2</del>	<del>2.8</del>	228.2	5.3	49.1	1.1
RP17	cyclic	3	6	2.1	407	6.5	-	7.6	-	6.6	4.5	49.3	<del>135.6</del>	<del>2.8</del>	173.7	3.5	30.0	0.6
RP18	cyclic	3	6	2.1	408	-	-	-	-	5.3	3.9	40.1	<del>118.7</del>	<del>3.0</del>	143.7	3.6	28.5	0.7
RP19	cyclic	3	6	2.1	412	-	7.0	6.6	-	6.3	6.3	52.5	<del>187.9</del>	<del>3.6</del>	221.4	4.2	44.0	0.8

**Table 2.** Optimization results computed using Schapery's model.

Test	$\dot{K}$ (kPa $\sqrt{\text{ms}^{-1}}$ )	$t_f$ (s)	$C_e \times 10^8$ (mN $^{-1}$ )	$C_{vp} \times 10^{10}$ (mN $^{-1}$ s $^{-1}$ )	$c$
RP15	2.912	68.2	3.330	1.061	1
RP16	2.808	42.8	3.845	0.974	1
RP17	2.750	49.3	2.637	0.512	1
RP18	2.960	40.1	1.861	0.209	1
RP19	3.579	52.5	2.775	0.938	1